

# Probing impulsive strain propagation with x-ray pulses

D. A. Reis<sup>1,2</sup>, M. F. DeCamp<sup>1</sup>, P. H. Bucksbaum<sup>1,2</sup>, R. Clarke<sup>1</sup>, E. Dufresne<sup>1</sup>, M. Hertlein<sup>1</sup>, R. Merlin<sup>1,2</sup>, R. Falcone<sup>3</sup>, H. Kapteyn<sup>4</sup>, M. Murnane<sup>4</sup>, J. Larsson<sup>5</sup>, Th. Missalla<sup>5</sup>, J. Wark<sup>6</sup>

<sup>1</sup>*Department of Physics, University of Michigan, Ann Arbor, MI 48109-1120*

<sup>2</sup>*Center for Ultrafast Optical Science, University of Michigan, Ann Arbor, MI 48109-2099*

<sup>3</sup>*Department of Physics University of California, Berkeley, CA 94720-7300*

<sup>4</sup>*JILA and Department of Physics, University of Colorado and National Institute of Standards and Technology, Campus Box 440, Boulder, CO 80309-0440*

<sup>5</sup>*Atomic Physics Division, Lund Institute of Technology, P. O. Box 118, SE-221 00, Lund, Sweden*

<sup>6</sup>*Department of Physics, Clarendon Laboratory, University of Oxford, Parks Road, Oxford, OX1 3PU, U.K.*

(October 31, 2018)

Pump-probe time-resolved x-ray diffraction of allowed and nearly forbidden reflections in InSb is used to follow the propagation of a coherent acoustic pulse generated by ultrafast laser-excitation. The surface and bulk components of the strain could be simultaneously measured due to the large x-ray penetration depth. Comparison of the experimental data with dynamical diffraction simulations suggests that the conventional model for impulsively generated strain underestimates the partitioning of energy into coherent modes.

78.47.+p 61.10.-i 63.20.-e

The absorption of ultrafast laser pulses in opaque materials generates coherent stress when the pulse length is short compared with time for sound to propagate across an optical penetration depth [1]. The resulting strain field consists of both a surface component, static on time scales where thermal diffusion can be ignored, and a bulk component that propagates at the speed of sound (coherent acoustic phonons). This strain is typically probed by optical methods that are sensitive primarily to the phonon component within the penetration depth of the light [1,2]. However, such methods give little information about the surface component of the strain, and, moreover, they are unable to give a quantitative measure of the strain amplitude.

Due to their short wavelengths, long penetration depths, and significant interaction with core electrons, x-rays are a sensitive probe of strain. We note that coherent lattice motion adds sidebands to ordinary Bragg reflection peaks due to x-ray Brillouin scattering if the momentum transfer is large compared to the Darwin width, equivalent to phonons of GHz frequency for strong reflections from perfect crystals. This effect was demonstrated many years ago with acoustoelectrically amplified phonons using a conventional x-ray tube [3].

With the recent availability of high brightness short-pulse hard x-ray sources, including third generation synchrotron sources and optical laser based sources [4–6], coherent strain generation and propagation can now be probed by x-ray methods in both the frequency and time domains. Recently, time-resolved diffraction patterns of cw ultrasonically excited crystals were obtained with a synchrotron source [7]. Other experiments have employed picosecond time-resolved x-ray diffraction to study transient lattice dynamics in metals [8], organic films [9], and impulsive strain generation and melting in semiconductors [10–14]. In particular Rose-Petruck *et al.* [10] demonstrated transient ultrafast strain propagation in GaAs by laser-pump x-ray-probe diffraction. In that experiment, x-rays were diffracted far outside the Bragg peak; however, no oscillations in the diffraction efficiency were detected, and the data were consistent with a unipolar strain pulse. In a similar experiment, Lindenberg *et al.* [13] detected oscillations in the sidebands for an asymmetrically cut InSb crystal using a streak camera. These oscillations were due to lattice compression and were probed for discrete phonon frequencies in the near surface regime.

In this Letter, we report on the modulation of x-ray diffraction from (111) InSb due to impulsively generated coherent acoustic phonons. We combined ultrafast pump-probe techniques with high resolution x-ray diffraction to build up a comprehensive time and frequency resolved picture of the induced strain. Because the x-rays probed deeper into the material than the laser penetration depth, the bulk, phonon component of the strain could be distinguished from the surface component as it propagated into the crystal. The data reveal both the compression and rarefaction of the associated strain wave. When compared with the standard model of strain production [15], our data suggest that the bulk component of the strain is twice the amplitude predicted by this model.

Both the allowed (strong) and nearly forbidden (weak) reflections from the 111 and 222 crystallographic planes of the face-centered cubic crystal were used. We believe this to be the first study of the effect of ultrasound on the diffraction in a nearly forbidden reflection offering important advantages in terms of the x-ray absorption depth and sensitivity to low frequency phonons.

The experiments were conducted at the Michigan/Howard/Lucent Technologies-Bell Labs collaborative access team (MHATT-CAT) 7ID insertion device beamline at the Advanced Photon Source (APS). The x-rays from the undulator were monochromatized by a cryogenically cooled silicon 111 double crystal monochromator. The photon energy was set to 10 keV and the bandwidth was approximately 1.4 eV. The x-rays were *p*-polarized with respect to the sample resulting in a reduction of the Bragg reflectivity compared to the reflectivity for *s*-polarization [16]. The scattering plane of the sample was also perpen-

dicular to that defined by the monochromator; however, the effect of dispersion on the reflections is expected to be small. The beam was collimated with slits before both the monochromator and the sample.

Ionization chambers monitored the x-ray flux before and after the sample. A silicon avalanche photodiode (APD), with a rise time of  $<3$  ns after preamplification [17], provided sufficient temporal resolution to gate a single x-ray pulse from the 150 ns pulse spacing in the APS singlets mode. The data were background subtracted to remove an angle dependent DC offset in the APD due to overshoot in the detector electronics from the previous x-ray bunch.

A commercial ultrafast 840 nm kHz Ti:sapphire laser impulsively excited large amplitude coherent acoustic phonon fields in the sample. The laser was phase-locked to a single x-ray pulse in the synchrotron with a timing jitter less than the x-ray pulse duration of 90 ps (FWHM). A digital phase shifter in the reference of the feedback loop provided a variable delay with 19 ps precision. The  $p$ -polarized laser pulse was focused to  $1 \times 1.5$  mm<sup>2</sup> at the sample, with an incident angle of 50 degrees, on the same side of normal as the incident x-ray pulse. The fluence was 10–12 mJ/cm<sup>2</sup>. The temporal structure of the laser consisted of two 70 fs pulses separated by less than a picosecond. This substructure is not expected to play a role in the strain dynamics.

Our results are summarized in Fig. 1. Figure 1(a) shows the measured time-resolved rocking curve for the symmetric 111 Bragg reflection following ultrafast laser excitation. The vertical axis is the time delay between the x-ray and the laser pulses. The time when the strain is first observed is defined as  $t = 0$ . The horizontal axis is the x-ray incident angle with respect to the center of the Bragg peak,  $\theta_0$ , in the laser-on condition. After the arrival of the laser pulse, the rocking curve broadens and shifts slightly towards smaller angles. During the first few hundred picoseconds, oscillations occur on the low angle side of the peak while on the high angle side there is both transient broadening and, for certain angles, decreased reflectivity. At longer delays only the broadening at negative angles persists, and no oscillations are evident.

Much of the behavior in Fig. 1(a) can be understood by kinematical diffraction. In the kinematic approximation, x-rays scattered at a given offset angle diffract from regions of material with appropriate crystallographic plane spacing. If the spacing between the planes is changing in time, then an offset  $\theta - \theta_B$  occurs due to Brillouin scattering of the x-rays from phonons of wavevector  $q = d^{-1}(\theta - \theta_B) \cot \theta_B$  where  $\theta_B$  is the Bragg angle and  $d$  is the unperturbed plane spacing [18]. Smaller angles thus correspond to lattice expansion and larger angles correspond to compression.

Oscillations occur in the diffracted signal because the phonons are coherent (since the stress is impulsive). A fast Fourier transform of the data for the expanded material gives a dispersion relation for the phonons consistent with the speed of sound for longitudinal acoustic modes propagating along the (111) direction. The temporal response of the material is expected to extend to 40 GHz assuming a 100 nm laser absorption depth and a 3880 m/s speed of sound; however the x-ray pulse length, timing jitter and dephasing (due to a small momentum spread of the x-rays) limit the detection of oscillations to approximately 10 GHz. Nonetheless higher frequency phonons are revealed by the existence of diffracted x-rays well outside the main Bragg peak corresponding to acoustic phonons up to approximately 40 GHz.

The longitudinal coherence length of the x-rays is  $0.9 \mu\text{m}$  allowing for interference between the x-rays diffracted from the strained and unstrained portions of the crystal. The absorption depth of 10 keV x-rays in InSb is approximately  $2.3 \mu\text{m}$  for the symmetric 111 reflection, corresponding to 600 ps at the acoustic velocity. In a strong reflection, the depletion of the input beam (extinction) limits the penetration depth. This extinction broadens the width of the diffraction peak and thus sets a lower limit on the phonon wavevector which can be resolved as a sideband. Strain persists on the expansion side well after the phonons traverse the absorption depth (as further indicated by the damping of any oscillations). This indicates that expanded material is left in the wake of the sound front due to surface heating from the laser. The slow decay of this surface strain occurs over a few hundred nanoseconds and is due to thermal diffusion; however, this is unimportant on the time scale of Fig. 1(a).

In order to study strain propagation over longer times, the x-ray must penetrate deeper into the bulk. At a fixed x-ray energy this requires either a weaker reflection or larger momentum transfer (larger Bragg angles). The 222 reflection for InSb is structurally forbidden except for a small difference in the scattering factors of the In and Sb atoms; the reflection is weak enough that extinction does not play a role, and the probe depth is limited by the absorption depth, which at 10 keV corresponds to approximately  $4.5 \mu\text{m}$ .

Figure 1(d) shows the time-resolved diffraction measurement of the symmetric 222 peak. In this data the time delay was scanned with 38 ps steps. The collimation slits were opened slightly wider than for the 111 data in order to increase the incident x-ray flux, at the expense of a slight decrease in the angular resolution. The peak of the rocking curve decreases in amplitude after laser excitation, with a time constant limited by our temporal resolution. After the initial drop, the diffraction efficiency again begins to build up, returning to the pre-strained value well before the arrival of the next laser pulse. In addition, after excitation there is a slight increase in the diffraction efficiency on the expansion side of the rocking curve. The signal to noise for the 222 reflection was insufficient to resolve any compression dynamics.

The data for both reflections are compared with simulations that model dynamical diffraction theory for a single reflection [19,20] in the presence of strain [21,22]. The lack of inversion symmetry in InSb is ignored, except in the determination of the structure factor for the 222 reflection. The rocking curves are calculated for a particular strain profile using the method given by Wie *et al.* [23]. The strain is calculated using the model of Thomsen *et al.* [15], who solved the elastic equations for an instantaneous and exponentially decaying stress due to short-pulse laser absorption. In our case this model predicts both a

0.51% strain across the 100 nm absorption depth and a 0.51% peak-to-peak bulk acoustic strain. Lindenberg *et al.* [13] found it necessary to include both an instantaneous stress due to the effect of free carriers on the deformation potential and a 12 ps delayed stress which they attribute to electron-phonon coupling. Similar delays are found in Ref. [10,12]. Such delays are on the order of the phonon propagation time across the laser penetration depth and are unresolved due to the temporal length of the x-ray probe.

Figures 1(c) and 1(f) show results of the simulations for the predicted 0.51% strain. To account for experimental resolutions, the calculations shown in Fig. 1(b) and Fig. 1(e) were convolved with Gaussians of 1.25 mdeg for 111, and 2.5 mdeg for 222, and 100 ps FWHM. In Fig. 1(b), a small incoherent 14 mdeg FWHM Gaussian pedestal was added to better reproduce the data (15% the amplitude of the peak).

While the simulations reproduce many of the features in the data, they underestimate the phonon contribution of the strain. This is particularly evident in the rocking curve of Fig. 2. To model the strain field more accurately, we allowed for separate partitioning of energy into surface and bulk components. A least squares fit of the  $\sim 6000$  data points for Fig. 1(a) yielded a 0.39% amplitude surface strain with a 0.76% peak-to-peak acoustic strain with a  $\chi_{dof}^2 = 0.5$ . By comparison, the model of Thomsen *et al.* gives  $\chi_{dof}^2 = 0.8$ . The relative statistical error in the strain determination is at the percent level, indicating that our data is limited by systematic errors.

We believe the data presented here to be the first x-ray diffraction probe of a bipolar ultrasonic pulse during its propagation into the bulk. We note that the time over which the pulse can be followed here was limited by absorption and extinction of the x-ray probe, and that in the Laue geometry the probe depth may be extended to the entire bulk of the crystal. Data collected with such a technique are currently under analysis for the case of a thick germanium single crystal. We further note that while the detection of the direct temporal response of the material was limited to 100 ps, shorter times could be probed due to the momentum sensitivity of x-ray diffraction. Improvements in the direct temporal resolution will allow for a more detailed study of the stress generation and the partitioning of energy into the lattice. Finally, extension of the techniques, discussed here, to the terahertz regime using coherent optical phonons may be used to slice sub-picosecond x-ray pulses from the somewhat longer pulse structure of third generation x-ray sources [24].

#### ACKNOWLEDGMENTS

We would like to thank A. Baron for providing us with the preamplifier circuit for the APD and E. Williams, S. Dierker and W. Lowe for their experimental support. This work was conducted at the MHATT-CAT insertion device beamline on the Advanced Photon Source and was supported in part by the U.S. Department of Energy, grants DE-FG02-99ER45743 and DE-FG02-00ER15031. Use of the Advanced Photon Source was supported by the U.S. Department of Energy, Basic Energy Sciences, Office of Energy Research, under Contract No. W-31-109-Eng-38. One of us (DR) acknowledges support from the National Science Foundation CUOS Fellows program.

- 
- [1] S. Akhmanov and V. E. Gusev, *Sov. Phys. Usp.* **35**, 153 (1992).
  - [2] A. C. Tam, *Rev. Mod. Phys.* **58**, 381 (1992).
  - [3] S. D. LeRoux, R. Colella, and R. Bray, *PRL* **35**, 230 (1975).
  - [4] M. M. Murnane *et al.*, *Science* **251**, 531 (1991).
  - [5] R. Schoenlein *et al.*, *Science* **274**, 236 (1996).
  - [6] R. Schoenlein *et al.*, *Science* **287**, 2237 (2000).
  - [7] K. D. Liss *et al.*, *Europhys. Lett.* **40**, 369 (1997).
  - [8] P. Chen, I. V. Tomov, and P. M. Rentzepis, *J. Chem. Phys.* **104**, 10001 (1996).
  - [9] C. Rischel *et al.*, *Nature* **390**, 490 (1997).
  - [10] C. Rose-Petruck *et al.*, *Nature* **398**, 310 (1999).
  - [11] C. Siders *et al.*, *Science* **286**, 1340 (1999).
  - [12] A. Chin *et al.*, *Phys. Rev. Lett.* **83**, 336 (1999).
  - [13] A. Lindenberg *et al.*, *Phys. Rev. Lett.* **84**, 111 (2000).
  - [14] A. Cavalleri *et al.*, *Phys. Rev. Lett.* **85**, 586 (2000).
  - [15] C. Thomsen, H. T. Grahn, H. J. Maris, and J. Tauc, *Phys. Rev. B* **34**, 4129 (1986).
  - [16] The peak reflectivity for *p*-polarization is  $\cos^2 2\theta_B$  that of the corresponding reflectivity for *s*-polarization. This amounts to a 11% (38%) reduction in the reflectivity for the 111 (222) reflection respectively.

- [17] A. Baron, Nucl. Instr. Meth. **A400**, 124 (1997).  
 [18] In the Bragg geometry there is a slight difference between the center of the Bragg peak,  $\theta_0$ , and the Bragg angle, defined through  $\sin \theta_B = \lambda/2d$ . This is due to the small difference in the index of refraction from unity.  
 [19] W. H. Zachariasen, *Theory of X-ray Diffraction in Crystals* (John Wiley and Sons, Inc., New York, 1945).  
 [20] B. Batterman and H. Cole, Rev. Mod. Phys. **36**, 681 (1964).  
 [21] S. Takagi, Acta Cryst. **15**, 1311 (1962).  
 [22] D. Taupin, Bull. Soc. Franç. Minér. Crist. **87**, 469 (1964).  
 [23] C. R. Wie, T. A. Tombrello, and J. T. Vreeland, J. Appl. Phys. **59**, 3743 (1986).  
 [24] P. Bucksbaum and R. Merlin, S.S. Comm. **111**, 535 (1999).

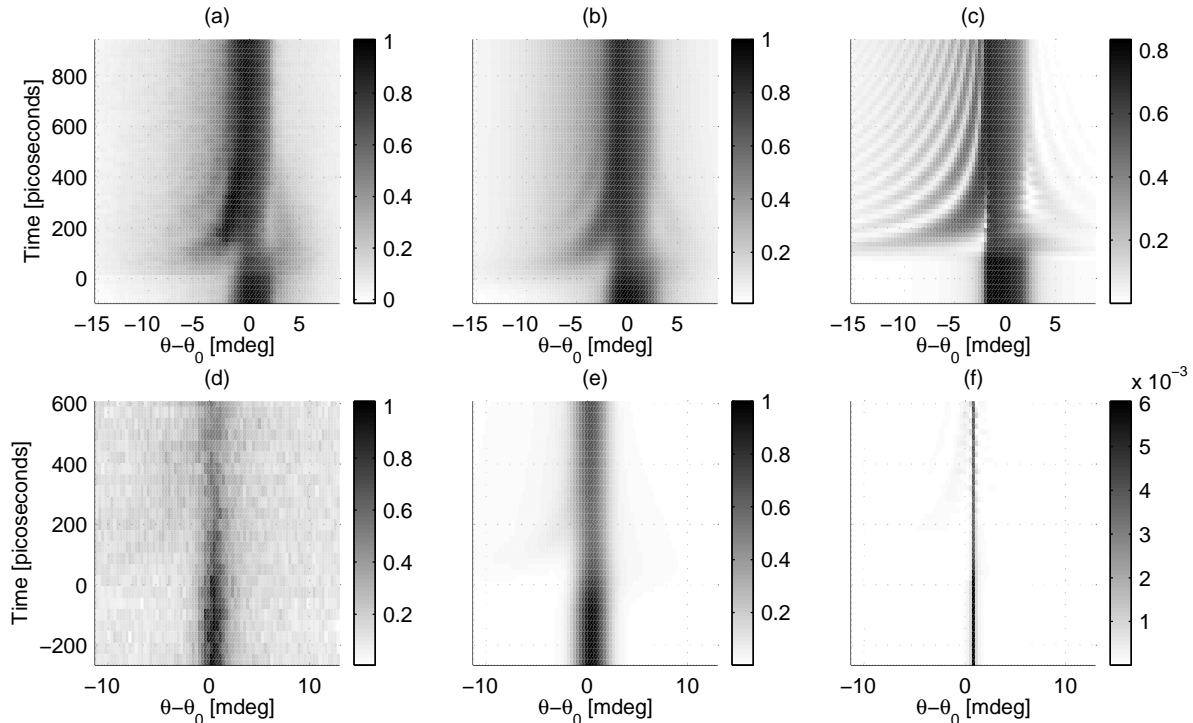


FIG. 1. Time-resolved rocking curves of impulsively strained InSb. (a),(d) Data and (b),(e) dynamical diffraction simulation for a 0.51% peak strain with a 100 nm laser absorption depth and a 100 ps, 1.25 mdeg (2.5 mdeg for the 222) FWHM Gaussian resolution functions (normalized to the peak unstrained signal); and (c),(f) Dynamical diffraction simulation for the reflectivity of a monochromatic x-ray pulse with ideal temporal resolution, all for the 111, 222 reflections respectively.

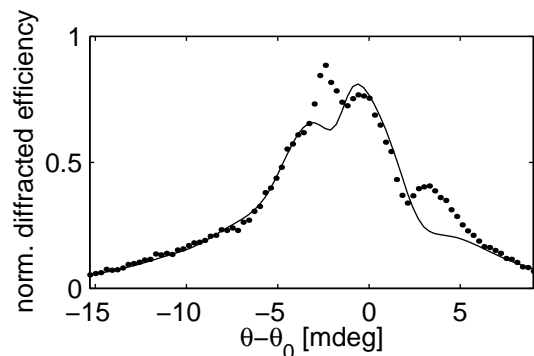


FIG. 2. Rocking curve of the 111 peak at 150 ps time delay (normalized to the peak unstrained value). The solid circles are the data and the line is the simulation. The discrepancy is interpreted as due to an excess of energy in coherent acoustic modes.